Journal of Pharmaceutical Analysis 2011;1(3):175–183

Xi'an Jiaotong University

Journal of Pharmaceutical Analysis

www.elsevier.com/locate/jpa
www.sciencedirect.com

ORIGINAL ARTICLE

Microfluidics-based assay on the effects of microenvironmental geometry and aqueous flow on bacterial adhesion behaviors

Yang Liu[a], Jian-Chun Wang[a], Li Ren[b], Qin Tu[a], Wen-Ming Liu[a], Xue-Qin Wang[b], Rui Liu[a], Yan-Rong Zhang[a], Jin-Yi Wang[a,b,c,*]

[a]*College of Science, Northwest A&F University, Yangling, Shaanxi 712100, China*
[b]*College of Veterinary Medicine, Northwest A&F University, Yangling, Shaanxi 712100, China*
[c]*Shaanxi Key Laboratory of Molecular Biology for Agriculture, Northwest A&F University, Yangling, Shaanxi 712100, China*

Received 10 May 2011; accepted 8 June 2011
Available online 22 July 2011

KEYWORDS

Microfluidic device;
Escherichia coli;
Adhesion behaviors;
Geometry;
Aqueous flow

Abstract A new microfluidic system with four different microchambers (a circle and three equilateral concave polygons) was designed and fabricated using poly(dimethylsiloxane) (PDMS) and the soft lithography method. Using this microfluidic device at six flow rates (5, 10, 20, 30, 40, and 50 μL/h), the effects of microenvironmental geometry and aqueous flow on bacterial adhesion behaviors were investigated. *Escherichia coli* HB101 pGLO, which could produce a green fluorescent protein induced by L-arabinose, was utilized as the model bacteria. The results demonstrated that bacterial adhesion was significantly related to culture time, microenvironment geometry, and aqueous flow rates. Adhered bacterial density increased with the culture time. Initially, the adhesion occurred at the microchamber sides, and then the entire chamber was gradually covered with increased culture time. Adhesion densities in the side zones were larger than those in the center zones because of the lower shearing force in the side zone. Also, the adhesion densities in the complex chambers were larger than those in the simple chambers. At low flow rates, the orientation of adhered bacteria was random and disorderly. At high flow rates, bacterial

*Corresponding author at: Colleges of Science and Veterinary Medicine. Northwest A&F University, Yangling, Shaanxi 712100, China. Tel./fax: +86 29 87082520.
E-mail address: jywang@nwsuaf.edu.cn (J.-Y. Wang).

Peer review under responsibility of Xi'an Jiaotong University.
doi:10.1016/j.jpha.2011.06.001

orientation became close to the streamline and oriented toward the flow direction. All these results implied that bacterial adhesion tended to occur in complicated aqueous flow areas. The present study provided an on-chip flow system for physiological behavior of biological cells, as well as provided a strategic cue for the prevention of bacterial infection and biofilm formation.

1. Introduction

Bacterial adhesion to surfaces, a general phenomenon, has important implications in daily life. Bacterial adhesion often occurs in implant surgeries, microbially induced corrosion, heat-exchange surfaces in food processing equipment, and natural environments [1,2]. For example, biomaterial-related infection starts with the adhesion of infectious bacteria, which is considered as one of the main causes of failure in implant surgery [3,4]. Bacterial adhesion to surfaces is also the onset of bacterial biofilm formation, which occurs on all surfaces exposed to an aqueous environment. Such environments include soft tissues, tooth surfaces, rocks, and ship hulls [5]. Bacterial biofilm is highly resistant to antimicrobial and fluid flows making it difficult to be eliminated [6–9]. The most effective and promising biofilm prevention method is to avoid the initial bacteria adhesion [10,11]. Therefore, research in the field of bacterial adhesion to surfaces has a great relevance in the prevention of biofilm formation.

Bacterial adhesion to surfaces usually presents in aqueous flows. An aqueous flow can promote the transport of microorganisms to surfaces and cause an increase in hydrodynamic detachment forces [12]. Some studies have shown that an increased fluid shearing force causes cells to bind more strongly, and results in a faster adhesion because of a higher mass transport. However, an overly high fluid flow prevents adhesion or even stimulates detachment when a critical flow limit is exceeded. This limit varies among strains and depends on the substratum material involved [5]. Two major stages of bacterial adhesion exist. The first is a reversible stage involving physico-chemical forces. The second is an irreversible stabilization phase involving both physico-chemical and chemical forces [1,13]. The irreversible phase implies a firmer adhesion of bacteria to the surface.

Flow displacement systems are important tools that mimic bacterial adhesion in fluid flow [5,14,15]. An adhesion experiment is conducted in flow displacement systems for three reasons: (1) to avoid external interference, (2) to allow the control and theoretical calculation of nutrient substance transport, and (3) to enable accurate measurements of the kinetic parameters of flow (such as flow rate and wall shearing rate) acting on adhering bacteria [5]. Recently, a new flow displacement system, the microfluidic flow system, has been utilized to investigate the behaviors of biological cells under various flow conditions [16]. The new system has many advantages over conventional benchtop systems. These advantages include low reagent and sample volume requirements, more accurate fluid flow simulation, precise kinetic control of the cellular microenvironment, and very low-cost [17]. Studies about the adhesion of animal cells in microfluidic flow systems have also advanced [18–20]. In the field of bacterial studies, microfluidic flow systems are used to construct a flow condition for bacterial culture wherein flow rate and shearing rate could easily be changed and calculated. Also, a few studies on bacterial adhesion in microfluidic devices have been reported [16,21–23]. Thomas [21] used rectangular microfluidic chambers to mimic *in vivo* conditions and study the effects of hydrodynamic shearing stress on bacterial adhesion. De La Fuente et al. [22] used a microfluidic chamber to assess drag forces and evaluate the adhesiveness of *Xylella fastidiosa* to glass surfaces. Mutations in type IV pilus-related genes were found to profoundly alter the speed of twitching motility in *X. fastidiosa*, particularly under the flow conditions in microfluidic devices [23]. Bahar et al. [16] demonstrated that type IV pili played critical roles in both the surface attachment and the biofilm formation of *A. citrulli* under flow conditions. These pili may also play important roles in the colonization and spreading of *A. citrulli* in xylem vessels under sap flow conditions.

The geometric structures of flow systems in natural environment are often complex. Such environments include the human body (blood vessels) or an artificial flow displacement system (e.g., water pipe). The geometry of an aquatic environment in flow systems may be greatly related to the physiological behavior of biological cells [24]. However, the reliability of using traditional flow displacement systems to study the influence of microenvironments on the adhesion behaviors of bacteria has not yet been established. The reason for this is that the geometries of microenvironments around bacterial cells are not easily controlled. Ironically, this disadvantage of a conventional flow displacement system is the advantage of a microfluidic flow displacement system. Microfluidic channels and chambers with various geometries can be easily designed, giving biological cells different microenvironments. To date, studies on cell behaviors using microfluidic flow systems have relatively progressed. A previous study on the impact of melanoma cell adhesion was performed under fairly low shearing conditions in a microfluidic flow system with a straight channel and a channel merging into a bifurcation [25]. Microfluidic channels with curved sections as well as sharp and rounded corners were designed to investigate the role of geometric features on the evolution of bacterial biofilm [26]. Microfluidic microchambers of distinct shapes and sizes, which allow bacteria escape, were used to investigate bacterial colonies. The development of bacterial colonies and the angle distribution on bacterial arrangements were suggested to be greatly influenced by the chamber shape [27]. Using differently shaped chambers, a bacterial microenvironment under flow conditions can be easily controlled. Microenvironment control is important in analyzing and demonstrating that the common phenomenon of bacteria adhesion is influenced by complex geometry in flow conditions. However, to the best of our knowledge, no relevant study on bacterial microenvironment geometry control has been reported thus far.

In the present study, a series of microchambers in a microfluidic system were distinctly designed to mimic the various geometries of flow conditions in a natural environment

such as blood or in an artificial device. The influence of flow system geometry on bacterial adhesion was demonstrated. The designed chambers had the same areas but different geometric shapes. The shapes included a circle and three equilateral concave polygons. The polygons had 8, 12, and 16 sides, as well as 4, 6, and 8 acute angles, respectively. Bacterial adhesion was observed using this microfluidic system. The bacterial strain used was *E. coli* HB101 pGLO, which could produce a green fluorescent protein (GFP) induced by L-arabinose. The density of bacterial adhesion was found to greatly correlate with chamber geometry and culture time. Different flow rates in this system were used to observe the changes in adhesion. Cell adhesion distribution and the orientation of adherent cells in these microchambers were also found to be influenced by the flow.

2. Materials and methods

2.1. Materials

RTV 615 poly(dimethylsiloxane) (PDMS) prepolymer and the curing agent were purchased from GE Silicones (Minato-ku, Tokyo). Surface-oxidized silicon wafers were from Shanghai Xiangjing Electronic Technology Ltd. (Shanghai, China). SU-8 2025 photoresist and developer were from Microchem (Newton, MA, USA). L-arabinose was purchased from Sigma–Aldrich (MO, USA). Ampicillin was from Amersco Inc. (Solon, OH, USA). Yeast extract and tryptone were from Oxoid Ltd. (Basingstoke, Hampshire, England). *E. coli* HB101 and the plasmid pGLO amp^r were supplied by Prof. Peng Chen of the College of Life Science, Northwest A&F University. All solvents and other chemicals were purchased from local commercial suppliers and were of analytical grade, unless otherwise stated. All solutions were prepared using ultra-purified water from a Milli-Q system (Millipore®).

2.2. Design and fabrication of the microfluidic device

The microfluidic device (Fig. 1) contains four centro-symmetric units. The units consisted of four parallel channels, each with an inlet and 16 outlets. Each channel had a circular and three equilateral concave polygonal microchambers. The polygons had 8, 12, and 16 sides, as well as 4, 6, and 8 acute angles, respectively. The parallel channels with microchambers were designed to enhance the consistency and reliability of the experimental data. The inlet for bacterial loading was circular and had a 500 μm radius. The main microchannels were 200, 100, and 50 μm wide, respectively, and were all 40 μm high. The detailed sizes of the four microchambers are shown in Fig. 1.

The microfluidic device was fabricated using soft lithography with PDMS [28,29]. The patterns were designed using the AutoCAD software. The microstructure and working units were printed at a resolution of 20,000 dots per inch (DPI) on a transparency film (MicroCAD Photomask Ltd., Suzhou, China) to be used as the photomask. A mold with 35-μm-high features was fabricated in a single step under ultraviolet (UV) light using an AZ 50XT photoresist (AZ Electronic Materials, Somerville, NJ, USA) on a BG-401 A mask aligner (7 mW/cm^2; CETC, China).

To fabricate the PDMS microfluidic device, the mold was exposed to chlorotrimethylsilane (TMCS, Alfa Aesar, Lancs, England) vapor for 3 min. The purpose of this exposure was to promote elastomer release after carrying out the baking steps.

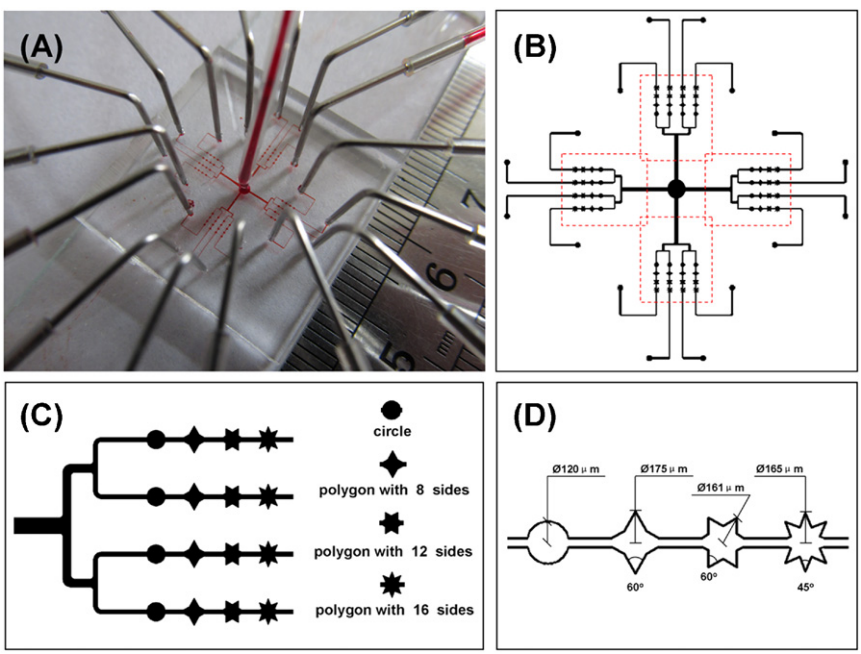

Figure 1 Configuration of the microfluidic device. (A) Optical image of the actual device. A ruler was employed to measure the size of the device. (B) Schematic representation of the functional circuit used for bacterial adhesion experiments. (C) Enlarged schematic representation of one unit of the main functional area of the microfluidic device corresponding to the dotted-line area in (A). (D) Details of the main channel and chambers. (For interpretation of the references to color in this figure, the reader is referred to the web version of this article.)

A mixture of PDMS (5 parts RTV615A:1 part RTV615B) was then poured onto the mold. After degassing, the mold was baked for 40 min at 85 °C, after which the PDMS flow layer structure was peeled-off from the mold. Through-holes were punched with a metal pin at the terminals of the inlet and outlet channels. The flow layer was irreversibly bonded onto a thin PDMS film (20 parts RTV615A:1 part RTV615B) on a glass slide and was baked overnight at 90 °C. The glass slide was pre-cleaned for 1 h in a piranha solution (H_2SO_4:H_2O_2=3:1, v/v) and was rinsed with Millipore ultra-pure water. Prior to using the slide, it was blow-dried with nitrogen (N_2).

2.3. *Preparation of the E. coli HB101 pGLO strain*

The *E. coli* HB101 pGLO strains were prepared using the electrotransformation technique, which is related to the two-step procedure of competent *E. coli* strain preparation and plasmid transformation. These procedures followed the methods previously reported [30,31]. The pGLO strain contains the jellyfish gene that codes the production of a GFP, and the β-lactamase gene that can be selected by placing ampicillin in the growth medium [32]. Cell stocks were stored in multiple aliquots with 15% glycerol in a liquid nitrogen tank at –196 °C prior to use. All subsequent procedures were performed at room temperature in a laminar flow hood to maintain the sterility of all reagents. Caution was used in handling all human biological materials.

2.4. *Bacterial cell culture and suspension preparation*

A single colony of *E. coli* HB101 from an overnight culture in Luria–Broth (LB) agar plates (5 g/L yeast extract, 10 g/L bactopeptone, 10 g/L sodium chloride, and 15 g/L agar) with 100 μg/mL ampicillin was inoculated into 150 mL of LB broth. The colony was continuously incubated for 12 h at 37 °C in a rotary shaker set at 200 rpm. The stationary-phase cell suspension was used for subsequent experiments. The cell density was determined using a normal plate-count method.

2.5. *Bacterial cell injection and adhesion assay in the microfluidic device*

The PDMS device was rinsed by flushing with 75% alcohol and Millipore ultra-pure water, and was sterilized overnight under UV light. The bacterial cell suspensions were then loaded into the microfluidic device for on-chip culture and sequential studies. After rinsing with water and drying with N_2, the *E. coli* HB101 pGLO suspensions in LB growth medium were injected into the microchambers. The suspensions were allowed to flow at 100 μL/h for several minutes at a desired cell density (2.0×10^9 CFU/mL). A cell culture medium with 0.4% (w/v) L-arabinose was then continuously provided by a flow (5, 10, 20, 30, 40, or 50 μL/h) of fresh supplemented LB growth medium. The microfluidic device was then incubated at 37 °C for a specific length of time (24, 48, or 72 h).

2.6. *Microscopy and image analysis*

An inverted microscope (Olympus, CKX41) with a CCD camera (QIMAGING, Micropublisher 5.0 RTV) was used to acquire phase-contrast and fluorescent images. Bacterial cell adhesion images were taken every 24 h after the unattached bacteria had been flushed with an LB growth medium flow (50 μl/L). The images were analyzed using the Image-Pro® Plus 6.0 software (Media Cyternetics, Silver Spring, MD). The adherent bacteria were counted in the center and side zones of each microchamber. To evaluate the reproducibility of the experimental results, each experiment was repeated at least three times. Statistical analyses were performed with the SPSS12.0 software (SPSS Inc.). Data are presented as mean ± SD.

3. Results and discussion

3.1. *Microfluidic device design and operation*

We previously studied *E. coli* responses to antibiotics in a zero-flow microfluidic device [17]. Based on this previous study, a microfluidic device with various geometry structures was designed and fabricated in the present study. The purpose was to investigate bacterial adhesion behaviors in various microenvironments and aqueous flow rates. The microfluidic device consisted of flow channels and chambers each with an inlet for sample loading (center circle in the device, Fig. 1), 16 outlets for waste exclusion, and 16 parallel channels with various test chambers (a circle and three equilateral concave polygons). For the purpose of parallel tests, four centro-symmetric units (red dot line in Fig. 1B) were employed and they were all connected to the central inlet. To evaluate bacterial adhesion ability, the total volume of all chambers was set at 1.6×10^{-3} μL.

3.2. *E. coli adhesion assay in the microfluidic device*

To effectively observe bacterial adhesion, a strain *E. coli* HB101 was transformed using a pGLO plasmid carrying a GFP. GFP synthesis by *E. coli* can be induced by L-arabinose. Under 0.4% (w/v) L-arabinose in LB liquid broth, the GFP-mediated fluorescence allowed for the visual identification of individual cells and quantitative analysis. After the bacterial cells were injected into the flow channels, most bacteria were retained in the center culture hole for growth and proliferation. The proliferation ensured sufficient cells in the medium flow to flush the substratum of the channels, which was a necessary condition of adhesion.

3.2.1. *Cell orientation in the microfluidic device*

The images taken in different microchambers at specific times were analyzed. The results showed that the orientation of *E. coli* cells attached at the microchamber bottom presented a uniform pattern under a proper flow rate of 30 μL/h after 48 h of culture (Fig. 2). In the circular chambers, cell orientation was almost completely parallel with the chamber sidewall. In the concave polygonal microchambers, the orientation of adhered *E. coli* was close to the side direction. Further observations revealed that this orientation was the same as the streamline of flow. Upon comparing the images of different flow rates, the orientation of *E. coli* was found to be greatly related to the flow. When the flow rate decreased, the parallelism of bacteria in the microchambers became weak. At 5 μL/h of flow rate and 48 h of culture time, cell orientation was more random and disorderly than at 30 μL/h (Fig. 2B). As

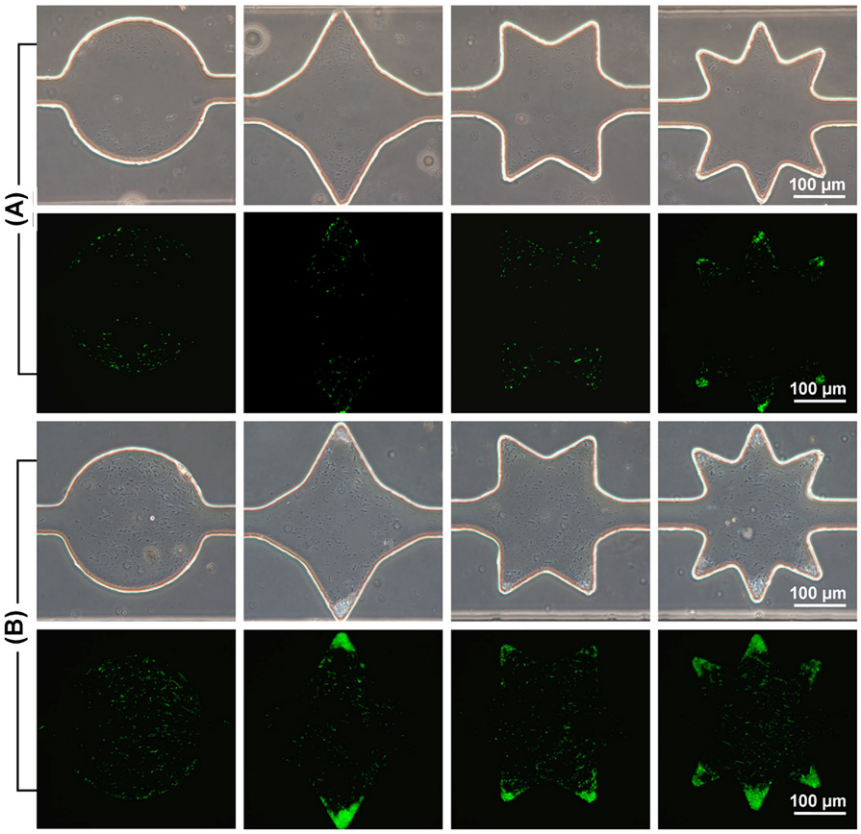

Figure 2 Time-dependent phase-contrast optical images and the corresponding fluorescence images of the four chambers with the *E. coli* HB101 pGLO strain. The images were taken during incubation in a growth medium flow with 0.4% L-arabinose. (A) Bacterial adhesion at a flow rate of 30 μL/h after 48 h of incubation at 37 °C. The orientation of adherent cells highly coincided with the flow direction. (B) Bacterial adhesion at a flow rate of 5 μL/h after 48 h of incubation at 37 °C. The orientation of the adherent cells was more disorderly than in (A).

medium flow rate increased, the cells attached and gradually became oriented with the flow direction. This finding was similar to a previous report [23] in which only a rectangular channel was employed. The adhesion behaviors of *E. coli* in circular or polygonal geometries have not yet been explored. A probable explanation of these behaviors is that the cells suffered from the lowest shear force when the rod was arrayed in the same direction as the laminar flow streamline. Otherwise, the force that is not parallel with the streamline compelled the bacteria to rotate to the parallel orientation. Under a low flow rate, a low shearing rate did not provide a sufficient force to change the rod direction. On the other hand, flow direction was greatly influenced by the sidewall of flow, which illustrated that the cell orientation was nearly parallel to the direction of the sides.

3.2.2. *Effect of culture time on bacterial cell adhesion*

In the current study, culture time was found to influence not only bacterial adhesion number but also location. Three incubation periods (24 h, 48 h, and 72 h) at 37 °C under a flow rate of 30 μL/h were used. The acquired phase-contrast and fluorescent images (Fig. 3) show that bacterial adhesion started at the chamber side. The entire PDMS substratum was then gradually covered, and adhesion number increased (Fig. 3A). This result is similar to the result of a previous study that used a straight channel [16]. The number and distribution of cells that remained attached to the substrate surfaces of interest following a period of incubation was used to evaluate bacterial adhesion. The results from such experiments are qualitative in nature [33–35].

To quantitatively analyze the effect of culture time on bacterial cell adhesion, the microchambers were artificially divided into two zones, the center and the side (top part, Fig. 4). The number of adherent cells in the center and sides, as well as the areas of the two zones in various microchambers were measured using the software Image-Pro Plus. For easy comparison, the bacterial adhesion numbers were converted to total cell populations per 10^4 μm^2. Fig. 4 (bottom, A, B, C, and D) shows the bacterial adhesion distribution in the microchambers with increased time. Cell adhesion was found to significantly increase both in the side and center zones, regardless of chamber geometry.

Further analysis demonstrated that cell densities in the side zones increased earlier than those in the center zones with increased culture time. Before 48 h, cell densities in the center zones increased very slowly compared with those in the side zones. However, the cell adhesion densities in the center zones increased abruptly after 48 h of culture much faster than the side zone. To explain the side-trended adhesion behavior of *E. coli*, a numerical simulation of the flow rate distribution in the microchambers was conducted using the software

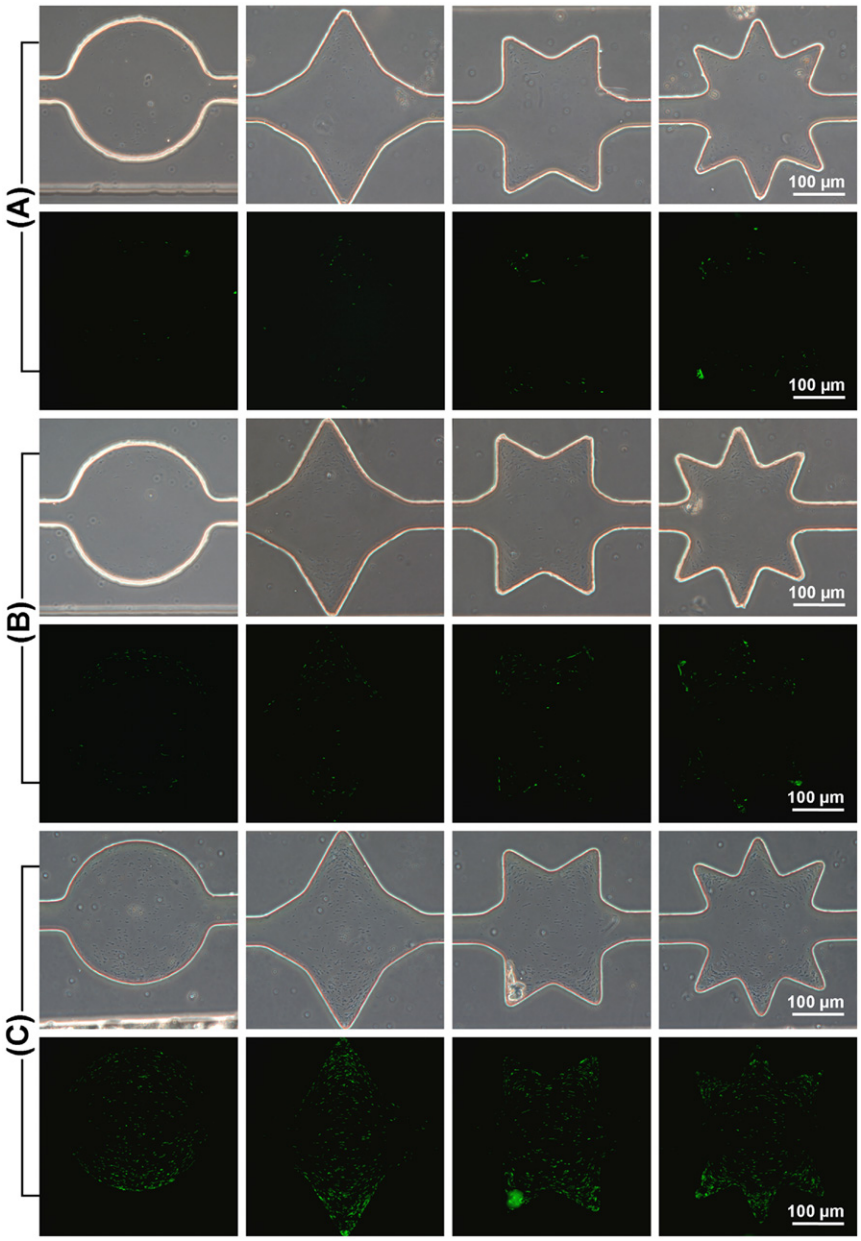

Figure 3 Time-dependent phase-contrast optical images and the corresponding fluorescence images of the four chambers. These images were taken, respectively, from three culture periods of 24 (A), 48 (B) and 72 h (C) at 37 °C and at a flow rate of 30 μL/h. The densities of the adhered cells distinctly increased.

CFD-ACE+(ESI group, Beijing, China). This simulation also corresponded to the distribution of shearing force in the microchambers. As shown in Fig. 5, the flow velocities (or shearing force) in the center zones were much higher than those in the side zones. Therefore, bacteria adhered in the side zones first, rather than in the center zones. After a specific culture time, bacterial adhesion turned to the center zones because of the confined space in the side zones.

3.2.3. Effect of geometry and flow rate on bacterial cell adhesion

To further investigate bacterial adhesion behaviors in various microenvironments and different flow rates, six flow rates (5, 10, 20, 30, 40, and 50 μL/h) were employed. The phase-contrast and fluorescent images of bacteria that adhered to the microchambers were taken after 48 h of culture at 37 °C. The adhered cell densities in both side and center zones were analyzed to evaluate the effects of flow and geometry on bacterial cell adhesion.

The relationship between flow rate (shearing rate) and adhered bacterial density is depicted in Fig. 6 for the six different flow rates and four geometries. Bacterial adhesion in the center zones is shown in Fig. 6A. The cell densities decreased with increased flow rates in the all four microchamber geometries. When flow rate increased beyond 30 μL/h, the cell densities were almost zero. This result verified that in an aqueous flow, a low shearing force promoted bacterial

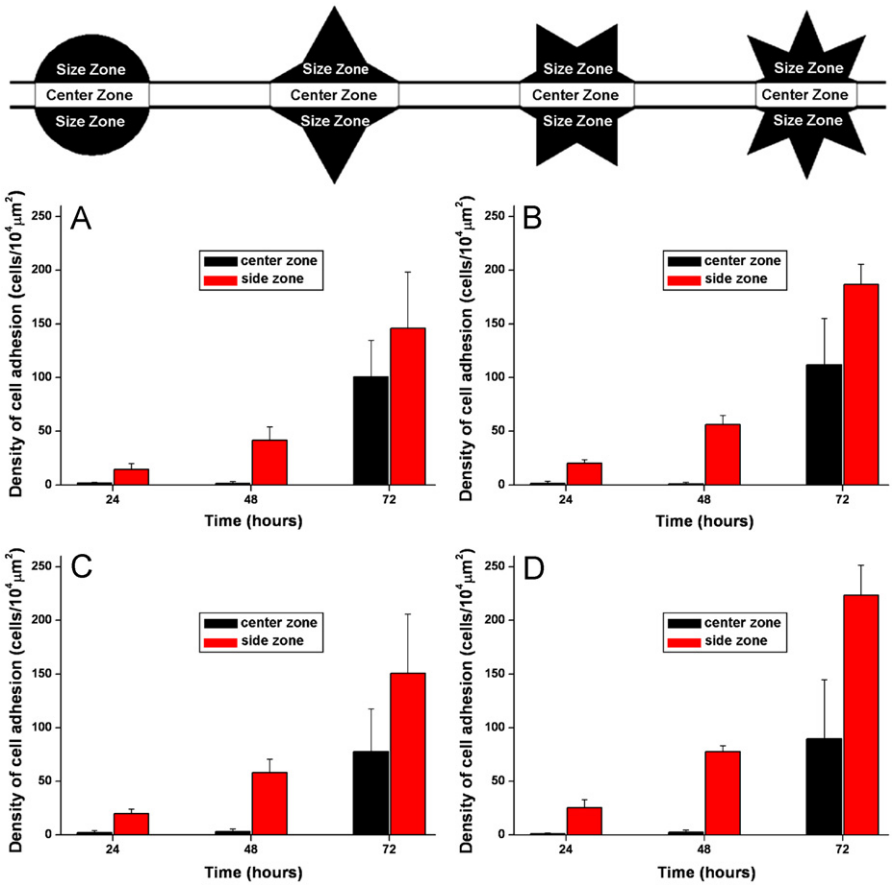

Figure 4 Top: the areas of interest (AOIs) of the microchambers by artificial definition. Bottom: the densities of adherent cells in the AOIs of circles (A) and polygons with 8 sides (B), 12 sides (C), and 16 sides (D). The densities were calculated by converting the adhesion numbers to total cell populations per 10,000 μm^2. Error bars represent standard deviations ($n \geq 3$).

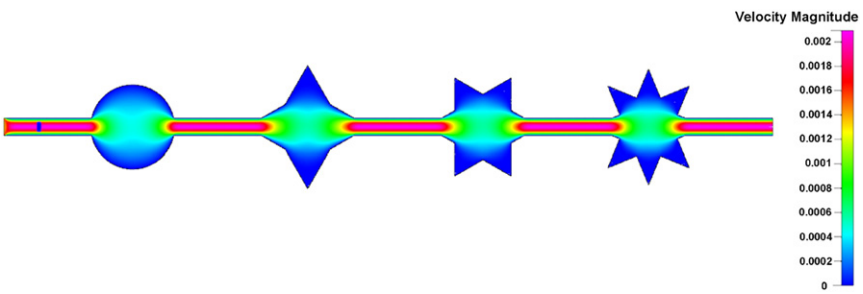

Figure 5 Flow velocity profiles in channels and chambers calculated by the commercial software CFD-ACE+, which correspondingly expressed shearing force distribution.

adhesion, whereas a very high shearing force led to detachment. This conclusion is the same as a previous report [36,37]. A comparison of cell adhesion phenomena among the geometric chambers revealed that cell densities in center zones were almost the same at a certain flow rate. A reasonable interpretation for this finding is that in the center zones, the shearing and flow velocities are the same (Fig. 5). As a result, the densities of the adherent cells were similar.

Fig. 6B shows the relationship between geometry (shearing rates) and adhered bacterial densities in the side zones. Similar to the center zones, cell densities also decreased with increased flow rates, although not in the same degrees for the four geometries. Under all flow rates, the cell densities in the side zones in the circular microchambers were markedly smaller than those in the other microchambers. In contrast, the cell densities were markedly larger in the polygonal microchambers with 16 sides than in the others. No significant difference was found between the polygonal microchambers with 8 and 12 sides. The same tendency among the four shapes and the six flow rates was found in the entire zone of the microchamber, as shown in Fig. 6C. Moreover, the cell adhesion densities in the side zones were distinctly larger than those in the center zones, as seen in Fig. 6A and B. All of these results indicated that bacterial adhesion occurs more in complex than in simple geometries (especially in the sidewalls) because of the lower shearing force.

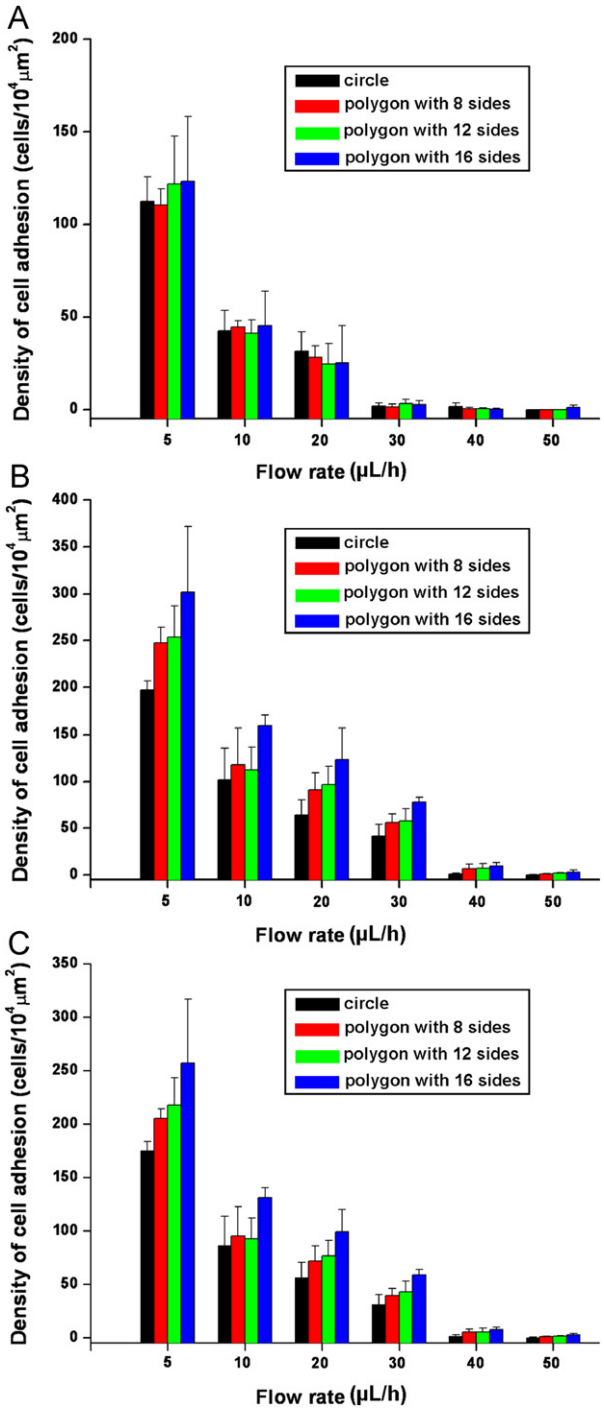

Figure 6 Densities of adhered *E. coli* cells at different flow rates and geometric chambers. The densities were calculated in the center zones, side zones, and chamber entirety. (A) Density of cells adhered in the center zone; (B) density of the cells adhered in the side zone; (C) density of the cells adhered in the entire chamber. Error bars represent standard deviations ($n \geq 3$).

4. Conclusion

A series of distinctly shaped microchambers in a microfluidic system were designed and fabricated using the soft lithography method. Using this microfluidic system, the effects of micro-environmental geometry and aqueous flow on bacterial adhesion behaviors were investigated. The results showed that bacterial adhesion greatly correlated with culture time, micro-environment geometry, and aqueous flow rate. At a low flow rate, the orientation of adhered bacteria was random and disorderly. With increased flow rate, the orientation of bacteria became close to the streamline and oriented with the flow direction. Moreover, adhered bacterial density increased with culture time. Initially, adhesion occurred at microchamber sides, and then the entire chamber is gradually covered with increased culture time. The adhesion densities in the side zones were larger than those in the center zones because of the low shearing force in the side zone. All these results implied that bacterial adhesion occurred in complicated aqueous flow areas. Therefore, our results provide a strategic cue for preventing bacterial infection and biofilm formation. Also, the adhesion densities in the complex chambers were larger than those in the simple chambers. The present work also demonstrated the use of a new microfluidics-based flow displacement system for further studying the physiological behaviors of bacteria.

Acknowledgments

This work was supported by the National Natural Science Foundation of China (Nos. 20975082 and 20775059), by the Ministry of Education of the People's Republic of China (NCET-08-0464), by the Scientific Research Foundation for Returned Overseas Chinese Scholars, by the State Education Ministry, and by the Northwest A&F University.

References

[1] K.C. Marshall, R. Stout, R. Mitchell, Mechanism of the initial events in the sorption of marine bacteria to surfaces, J. Gen. Microbiol. 68 (3) (1971) 337–348.
[2] A. Rochex, J.-J. Godon, N. Bernet, et al., Role of shear stress on composition, diversity and dynamics of biofilm bacterial communities, Water Res. 42 (20) (2008) 4915–4922.
[3] M.R. Nejadnick, H.C. van der Mei, W. Norde, et al., Bacterial adhesion and growth on a polymer brush-coating, Biomaterials 29 (30) (2008) 4117–4121.
[4] W. Zimmerli, F.A. Waldvogel, P. Vaudaux, et al., Pathogenesis of foreign body infection: description and characteristics of an animal model, J. Infect. Dis. 146 (4) (1982) 487–497.
[5] H.J. Busscher, H.C. van der Mei, Microbial adhesion in flow displacement systems, Clin. Microbiol. Rev. 19 (1) (2006) 127–141.
[6] J.W. Costerton, P.S. Stewart, E.P. Greenberg, Bacterial biofilms: a common cause of persistent infections, Science 284 (5418) (1999) 1318–1322.
[7] Y.J. Eun, D.B. Weibel, Fabrication of microbial biofilm arrays by geometric control of cell adhesion, Langmuir 25 (8) (2009) 4643–4654.
[8] T.F. Mah, G.A. O'Toole, Mechanisms of biofilm resistance to antimicrobial agents, Trends Microbiol. 9 (1) (2001) 34–39.
[9] M.R. Benoit, C.G. Conant, C. Ionescu-Zanetti, et al., New device for high throughput viability screening of flow biofilms, Appl. Environ. Microbiol. 76 (13) (2010) 4136–4142.
[10] G. Cheng, Z. Zhang, S. Chen, et al., Inhibition of bacterial adhesion and biofilm formation on zwitterionic surfaces, Biomaterials 28 (29) (2007) 4192–4199.
[11] G.W. Charville, E.M. Hetrick, C.B. Geer, et al., Reduced bacterial adhesion to fibrinogen-coated substrates via nitric oxide release, Biomaterials 29 (30) (2008) 4039–4044.

[12] N.P. Boks, W. Norde, H.C. van der Mei, et al., Forces involved in bacterial adhesion to hydrophilic and hydrophobic surfaces, Microbiology 154 (10) (2008) 3122–3133.
[13] A. Terada, A. Yuasa, T. Kushimoto, et al., Bacterial adhesion to and viability on positively charged polymer surfaces, Microbiology 152 (12) (2006) 3575–3583.
[14] J.M. Meinders, H.C. van der Mei, H.J. Busscher, et al., Deposition efficiency and reversibility of bacterial adhesion under flow, J. Colloid Interface Sci. 176 (2) (1995) 329–341.
[15] M.G. Katsikogianni, Y.F. Missirlis, Bacterial adhesion onto materials with specific surface chemistries under flow conditions, J. Mater. Sci.: Mater. Med. 21 (3) (2010) 963–968.
[16] O. Bahar, L. De La Fuente, S. Burdman, Assessing adhesion, biofilm formation and motility of Acidovorax citrulli using microfluidic flow chambers, FEMS Microbiol. Lett. 312 (1) (2010) 33–39.
[17] P. Sun, Y. Liu, J. Sha, et al., High-throughput microfluidic system for long-term bacteria colony monitoring and antibiotic testing in zero-flow environments, Biosens. Bioelectron. 26 (5) (2011) 1933–1999.
[18] K.V. Christ, K.B. Williamson, K.S. Masters, et al., Characterization of the effect of geometry on single cell adhesion strength using a microfluidic device, IMECE2007 10 (A and B) (2007) 809–810.
[19] E. Gutierrez, B.G. Petrich, S.J. Shattil, et al., Microfluidic devices for studies of shear-dependent platelet adhesion, Lab Chip 8 (9) (2008) 1486–1495.
[20] C.G. Conant, M.A. Schwartz, T. Nevill, et al., Platelet adhesion and aggregation under flow using microfluidic flow cells, J. Vis. Exp. 32 (2009) 1644.
[21] W.E. Thomas, Using a laminar flow system to explain shear-enhanced bacterial adhesion, in: Proceedings of ICMM2005, Third International Conference on Microchannels and Minichannels, Toronto, Ontario, Canada, (Pt A), June 13–15, 2005, pp. 751–759, 〈http://www.asme.org/terms/Terms_Use.cfm〉.
[22] L. De La Fuente, E. Montanes, Y. Meng, et al., Assessing adhesion forces of type I and type IV pili of *Xylella fastidiosa* bacteria by use of a microfluidic flow chamber, Appl. Environ. Microbiol. 73 (8) (2007) 2690–2696.
[23] L. De La Fuente, T.J. Burr, H.C. Hoch, Mutations in type I and type IV pilus biosynthetic genes affect twitching motility rates in *Xylella fastidiosa*, J. Bacteriol. 189 (20) (2007) 7507–7510.
[24] E. Lauga, A.D. Stroock, H.A. Stone, Three-dimensional flows in slowly varying planar geometries, Phys. Fluids 16 (8) (2004) 3051–3062.
[25] M.A. Fallah, V.M. Myles, T. Krüger, et al., Acoustic driven flow and lattice Boltzmann simulations to study cell adhesion in biofunctionalized μ-fluidic channels with complex geometry, Biomicrofluidics 4 (2) (2010) 024106.
[26] R. Rusconi, S. Lecuyer, L. Guglielmini, et al., Laminar flow around corners triggers the formation of biofilm streamers, J. R. Soc. Interface 7 (50) (2010) 1293–1299.
[27] H. Cho, H. Jönsson, K. Campbell, et al., Self-organization in high-density bacterial colonies: efficient crowd control, PLoS Biol. 5 (11) (2007) e302.
[28] T. Thorsen, S.J. Maerkl, S.R. Quake, et al., Microfluidic large-scale integration, Science 298 (5593) (2002) 580–584.
[29] J.C. McDonald, D.C. Duffy, J.R. Anderson, et al., Fabrication of microfluidic systems in poly(dimethylsiloxane), Electrophoresis 21 (1) (2000) 27–40.
[30] N. Eynard, S. Sixou, N. Duran, et al., Fast kinetics studies of *Escherichia coli* electrotransformation, Eur. J. Biochem. 209 (1) (1992) 431–436.
[31] W.J. Dower, J.F. Miller, C.W. Ragsdale, et al., High efficiency transformation of *E. coli* by high voltage electroporation, Nucleic Acids Res. 16 (13) (1988) 6127–6145.
[32] M. Wong, M. Wright, J.M. Woodley, et al., Enhanced recombinant protein synthesis in batch and fed-batch *Escherichia coli* fermentation based on removal of inhibitory acetate by electrodialysis, J. Chem. Technol. Biotechnol. 84 (9) (2009) 1284–1291.
[33] M.R. Nejadnik, H.C. van der Mei, H.J. Busscher, et al., Determination of the shear force at the balance between bacterial attachment and detachment in weak-adherence systems, using a flow displacement chamber, Appl. Environ. Microbiol. 74 (3) (2008) 916–919.
[34] M. Hermansson, The DLVO theory in microbial adhesion, Colloids Surf. B: Biointerfaces 14 (1) (1999) 105–119.
[35] Y.L. Ong, A. Razatos, G. Georgiou, et al., Adhesion forces between *E. coli* bacteria and biomaterial surfaces, Langmuir 15 (8) (1999) 2719–2725.
[36] C.E. Christersson, P.O. Glantz, R.E. Baier, et al., Role of temperature and shear forces on microbial detachment, Scand. J. Dent. Res. 96 (2) (1988) 91–98.
[37] M.G. Katsikogianni, Y.F. Missirlis, Interactions of bacteria with specific biomaterial surface chemistries under flow conditions, Acta Biomater. 6 (3) (2010) 1107–1118.